Experimental and Numerical Study of the Reinforced Panels Subjected to Tensile Loading: Crack Stoppers

Panagiotis J. Charitidis[1*], Dimitrios A. Zacharopoulos[2]

[*1]School of Environmental Engineering, Democritus University of Thrace, Xanthi, Xanthi, Greece-67100
[2]School of Engineering, Democritus University of Thrace, Xanthi, Xanthi, Greece-67100
*Corresponding Author

Received: 03 October 2021/ Revised: 11 October 2021/ Accepted: 16 October 2021/ Published: 31-10-2021

Abstract— *The present study concerns with the experimental and numerical investigation of crack stoppers ahead of an edge crack in panels subjected to tensile loading. Two different patches (rectangular and semi-annular patches) have been analyzed. The patches (aluminium and steel) are placed at different distance from the crack, symmetrically on both sides of the panel and at a finite distance ahead of the crack tip. A finite distance ahead of the crack tip reveals that depending on the distance, the crack tip could remain straight or curve. In such cases, the crack could either be arrested, run through or run around the reinforcements. Moreover, the degree of instability is reflected by an index parameter that accounts for the effect of load, geometry and material properties. Moreover, a geometrically nonlinear, two-dimensional (2D) finite element analysis (Comsol Multiphysics) has been employed to determine the local energy intensity. It would be of special interest to know whether the crack would run straight and arrest at the patch regardless of the other variables. The ultimate goal for straight crack path is to produce sufficient low local energy intensity. This gives a significant advantage because as the local energy intensity is increased, crack would tend to curve and lead to complete fracture of the patched specimens. It is equivalent of moving the patch closer to the crack tip. The predictions made from the strain energy density theory, as well as, there is a good agreement between finite element results and experimental findings.*

Keywords— Comsol multiphysics, crack stoppers, energy density, reinforcement patch.

I. INTRODUCTION

A challenging problem which arises during production are the defects in structural components. A practice often used is to repair the cracked members by bonding patches to redirect the load path [1-8] to reduce the local stress or energy intensity level below critical. However, it is well known, that unlike the repair patches [9–15], which are used when fatigue cracks are detected, crack retarders will be part of the original aircraft structure and subjected to operational loads and environments throughout the entire service life. It means that aircraft structures could be safer, lighter, and cheaper. Especially, by using adhesively bonded composite patches, which are more efficient and much less damaging to the parent structure than standard repairs based on mechanically fastened metallic patches [16].

The development of bonded composite repair technology has been accelerated by many researches in the aerospace industry in the interests of increasing the service life and reducing the repair cost [17–19]. Composite repair has taken numerous roles on military aircraft, such as reinforcement in areas where stress corrosion cracking can occur, as on the lower surface of the wing pivot on a U.S. Air Force F-111, or fatigue cracking around a fuel decant hole on a Royal Australian Air Force (RAAF) Mirage III. On commercial aircraft, the use of composite repairs is in early stages [20]. On the other hand, one of the key issues in aircraft failure is the presence of multiple cracks in a local area, known as multisite damage (MSD). Analysis of the repair of MSD has been proposed by Park et al., [21] by placing a patch over a cracked pin-loaded fastener hole.

In addition to knowledge of the detailed stresses near the defects or cracks, a suitable failure criterion is needed to determine the effectiveness of the repair process. Improper repair could cause more harm than good. This has been known in the aircraft repair industry. The classical failure criteria are not adequate because they could not correct local and global failure in a constant manner to include the combined effects of loading rate, geometry and material. The concept of stable failure is pertinent, which means that structures in order to be safe, must be designed in a way that cracks are developing smoothly and

slowly according to the increase in loading rate. The damage should become so obvious that repair be made prior to catastrophic failure. More specifically, the period of stable crack growth should be prolonged. To this end, the local and global stationary values of the strain energy density function can be used mostly effectively for this purpose. While the basic concept of this approach can be found in [22-24], applications to a host of practical problem are given in [25-31]. The site of crack initiation can be determined without the need to assume an initial crack; it is taken to coincide with regions where dilatation is largest in comparison with distortion. These regions can be sorted out automatically from the maximum and minimum value of the strain energy density function. Hence, the approach applies equally well to nonlinear materials [31] where the dilatational and distortional components of the strain energy density function can no longer be separated as in the case of linear elasticity. To illustrate the application of these criteria, it suffices to consider linear elasticity.

Another interesting parameter is the stress intensity factor. The determination of the stress intensity factor (SIF) at the crack tip for any loading mode (K_I, K_{II}, K_{III}) is one of the means for analyzing the performance of the bonded patch in repairing cracks [32–39]. On the other hand, several authors computed the SIF at the crack tip of repaired cracks under mechanical loading [40-50]. Nowadays, stress intensity factor can be calculated with great accuracy by using finite element software's. A quite interesting example is Bachir Bouiadjra et al. [51] report, where for a single-patch repair analysis the increase of the patch thickness by about 50% reduces the stress intensity factors at the same order. They suggested that in order to increase accuracy multiple layers of bonded composite patch, must be used.

Among the means that can strengthen these ideas is the use of the double-sided symmetric patch. Many authors showed the advantage of the double-sided symmetric patches experimentally and numerically, among them, one can quote: Ting et al. [52], Bachir Bouiadjra et al. [32, 43, 53] and Belhouari et al. [47]. The literature review [32, 43, 47, 52, 53] shows that the double-sided symmetric patch reduces more the stress intensity at the crack tip, while it annuls the bending effect due to the eccentricity of the patch. The single edge crack configuration is depicted in this work where patches of different shape, size, location and material are bonded to the specimens. Evaluated are the corresponding strain energy density functions from which the location of the local and global stationary value can be determined. This yield a single parameter that would reflect the combine influence of the load, geometry and material. The magnitude of this parameter determines the overall stability or instability of the patched structure. Experiments are then performed for steel and aluminum patches of different size and patch location to study whether the analytical findings would yield the same results.

II. REINFORCEMENTS AND MATERIALS

2.1 Geometry Configuration

The testing configuration is a rectangular panel with an edge crack of length a as shown in Fig. 1. Following, Zacharopoulos report [54], a rectangular panel with a certain dimension was selected. The dimensions of the specimen were as following; width W=6cm; a height 2H=20cm and thickness t_P=0.24cm. The panel is subjected to a uniform stress (σ = 10 MPa) which is applied in the y-direction, that is normal to the crack which coincides with the x-axis. A central crack of length 2a perpendicular to the loading axis exists in the plate. The rectangular and annular patch have dimensions of r = 1 cm, b = 1 cm and $t_A = t_S$ = 0.1cm where **A** stands for aluminum and **S** for steel. The parameter d in Fig. 1 is used to denote the distance from the patch to the crack tip.

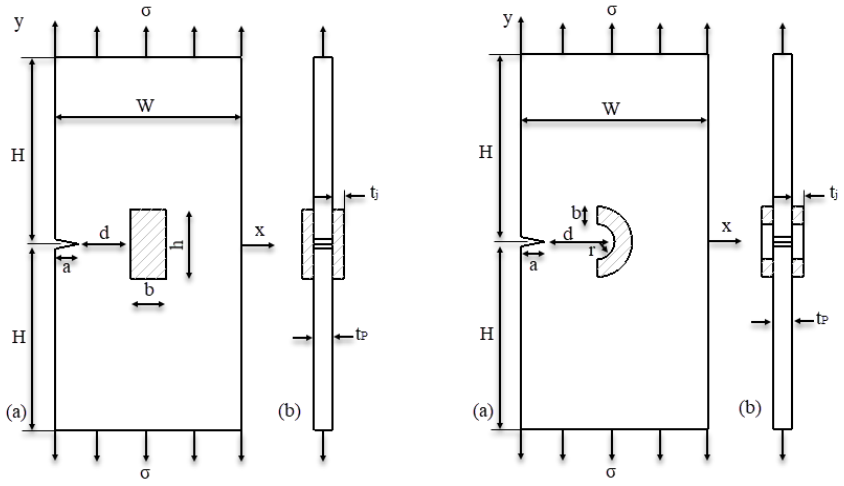

FIGURE 1: A test specimen configuration: (a) plane view; (b) thickness view

2.2 Material and Fracture Properties

Two different patches materials (aluminium and steel) were considered in this work, while the panel is made of plexiglass. The mechanical and fracture properties of the materials are given in Table 1. The effect of the patches and panel can be regarded to behave as a unit with an effective stiffness.

TABLE 1
MECHANICAL AND FRACTURE PROPERTIES OF PANELS AND PATCHES [54]

Material	Young's Modulus E (MPa)	Poisson's Ratio, ν	Yield Strength σ_y (MPa)	Tensile Strength σ_f (MPa)	Critical Stress Int. Factor K_{IC}(MPa $m^{1/2}$)
Plexiglass	3400	0.31	---	85.0	1.19
Aluminum	71000	0.33	72.0	150.0	---
Steel	210000	0.28	200.0	370.0	---

Let E* denote the effective Young's modulus given by (1)

$$E^* = \frac{t_P E_p + 2t_j E_j}{t_P + 2t_j} \tag{1}$$

where E_P and E_j are, respectively, the Young's moduli of plexiglass and patches. The same applies to the estimate of an effective Poisson's ratio (2):

$$\nu^* = \frac{t_P \nu_p + 2t_j \nu_j}{t_P + 2t_j} \tag{2}$$

In which ν_p and ν_j stand for Poisson's ratio of the panel and patches, respectively. Based on Eqs. (1) and (2), the effective values E* and ν* are calculated and given in Table 2.

TABLE 2
EFFECTIVE PROPERTIES OF E* AND ν*[54]

Material	E (MPa)	ν
Plexiglass/ Aluminum	34000	0.309
Plexiglass/Steel	97000	0.291

Furthermore, for plexiglass, the value $r_c = 2.8 \times 10^{-3}$ cm is used to compute for K_{IC} in Table 1 from Eq. (2).

2.3 Failure Path

It is well known that for a body with an initial crack, the site of maximum strain energy density function would coincide with the crack tip. That means, there is a location where the volume changes, making the strain energy per unit volume be smallest one dW/dV. In order to intedify the location, consider a typical location P_j with a local coordinate (x_j, y_j) (fig. 2). The distance r_o varies as a function of the angle θ_j. As the distance increases the subscript L would be different as the position of the reference axis changes. That means, for every value, another value of $(dW/dV)_{min}^{max}$ would be found when reference is made to the global coordinates (X, Y) in Fig. 2.

Moreover, as the L tends to G, the phenomenon would be called as a global, and it could be tested also experimentally. Hypothesis of the Maximum Gradient of the Strain Energy Density (HMG of SED), which predicts with great accuracy the directional accuracy has been applied to brittle materials or materials that behave in brittle way (elastic-plastic materials) [55]. There is also a considerable amount of literature on strain energy density theory [22-24], but this study, will be limited to fracture only, by using also finite element analysis (Comsol Multiphysics) in order to verify the experimental results. As for the instability index, namely l [2,22-26], it could be taken approximately as a straight-line distance between L and G. This would provide an indication of the fracture trajectory at which stable growth would terminate at G where the onset of rapid fracture would start. For a more precise estimate of the crack path, small increments of crack growth can be taken to obtain the full curvature of the path from L to G as shown in Fig. 1. Such analysis for crack trajectories emanating from the tip of an angle crack can be found in [56].

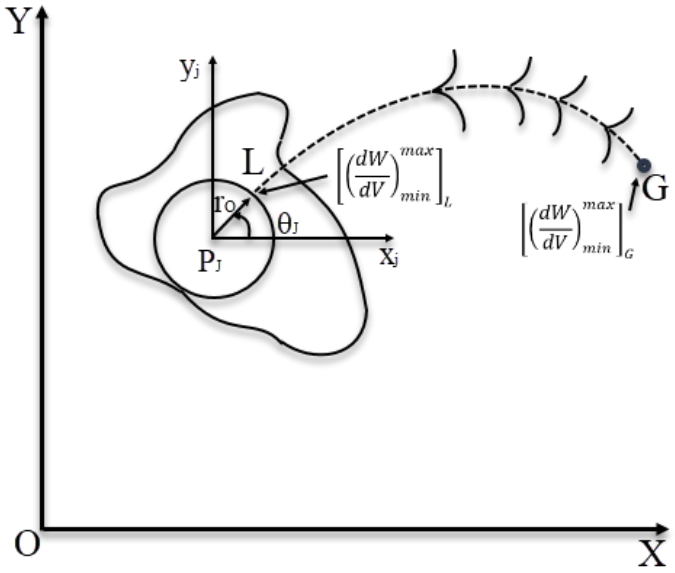

FIGURE 2: System ability: local and global stationary values of strain energy density.

III. EXPERIMENTAL PROCEDURE

A fretsaw is first used to make a cut in the plexiglass and a finer cut is then made using a razor blade. The specimen is loaded under control-displacement condition and the edge notch is allowed to propagate stably until the desired length is reached. Both aluminum and steel are used to make the rectangular and circular patches with $t_A = t_S = 0.1$cm. The planar dimensions for the former are b = 1 cm and h = 2 and 4 cm while for the latter r = b = 1 cm. These patches are bonded to both sides of the panel using a thin glue film with shear strength of 21.0MPa. Such strength is sufficient to transfer the load from the plexiglass to the metallic patches without debonding.

Moreover, the specimens were tested under load-controlled condition in a 60 kN Shenck hydraulic machine. Loading rates are increased to observe whether the crack propagation characteristics would alter for different patch length. All results of critical stresses for patched panels are normalized with reference to the fracture stress of the unreinforced panel with an edge crack. Hence, the ratio would always be greater than unity. While discrete test data points are obtained, all analytical results are given by solid curve.

IV. FINITE ELEMENT ANALYSIS

To ensure there is no relative motion between the plate and the patch, both of them are constrained by tying with the adhesive layer. The finite element analysis was performed using Comsol Multiphysics [57]. It has been applied to solve for the stresses and strain energy density functions. Numerical results are obtained for the rectangular and semicircular patches, the dimensions of which have already been given. For the aluminum patch $E_A/E_P = 21$ while for the steel patch $E_S/E_P = 62$. The distance d = 1, 2 and 3 cm for a = 1 and 2 cm (rectangular patches).

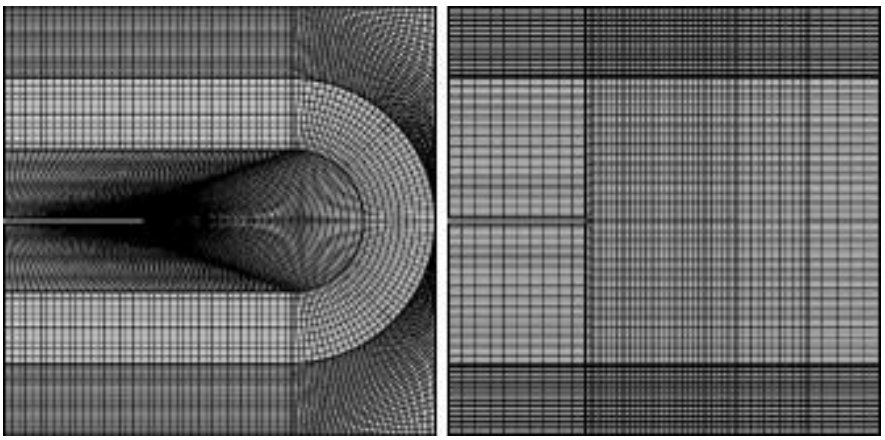

FIGURE 3: Finite element mesh density for semi-circle and rectangular reinforcement specimen [145,535 elements for all cases]

4.1 Rectangular Patches

Plotted in Figs. 4-7 are the normalized critical stresses σ_j/σ_c (j = A, S) as a function of the distance d. All curves tend to unity at about d = 3cm at which point the crack has no interaction with the patch. The critical stress σ_j and σ_c correspond to the panel with and without the patch, respectively. First of all, the test data agree well with the solid curves obtained from the strain energy density theory. The results in Figs. 3 and 4 correspond to those for the aluminum and steel patch, respectively. Note that when the patch size is doubled, the critical stress ratio σ_j/σ_p for aluminum and steel patch increases 35% and 45%, respectively, for patch location of d = 1 cm (a=1cm). The effect of reinforcement is significant and is expected to decrease with increasing d. The increase of critical stress due to enlargement of the patch size are clearly shown in Figs. 4 and 5 for the case of a = 1 cm. Similar results are displayed in Figs. 6 and 7 for a = 2cm.

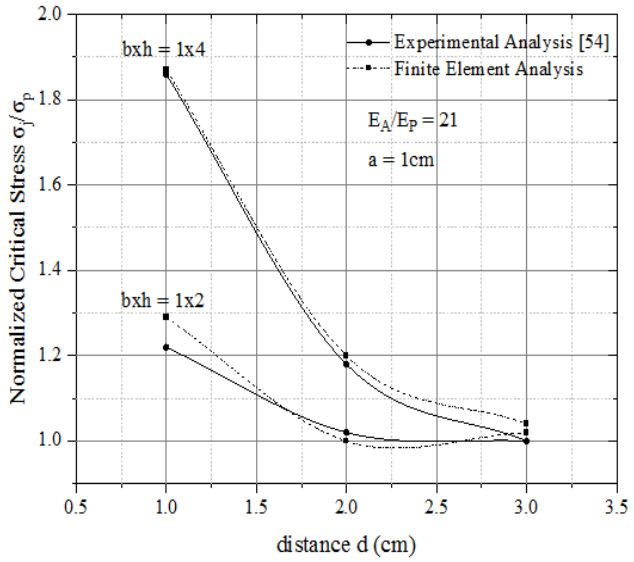

FIGURE 4: Normalized critical stress versus distance d for aluminum rectangular patch and a=1cm. (Note: a in the text is visualized as ``a'' in the figures throughout.)

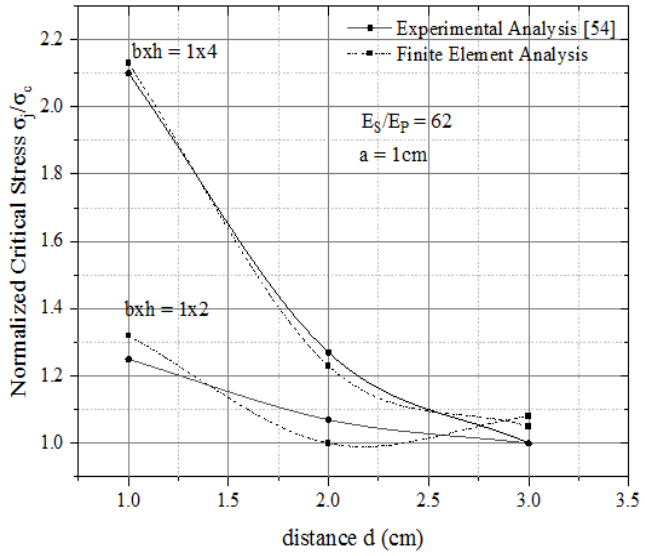

FIGURE 5: Normalized critical stress versus distance d for steel rectangular patch and a=1cm.

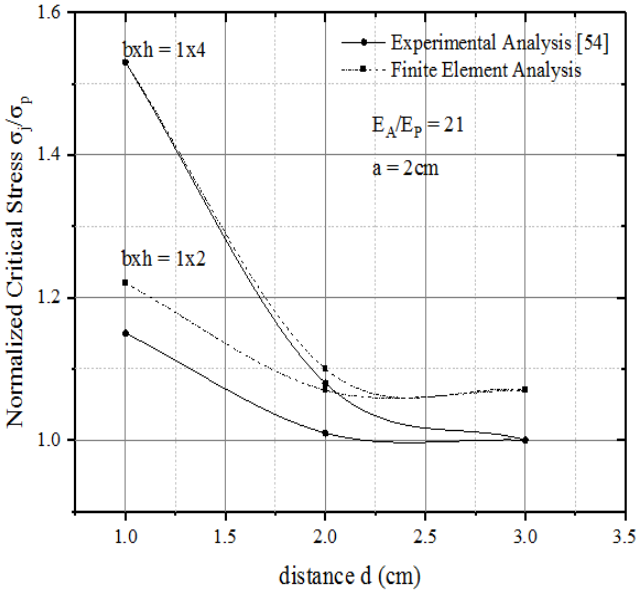

FIGURE 6: Normalized critical stress versus distance d for aluminium rectangular patch and a=2cm.

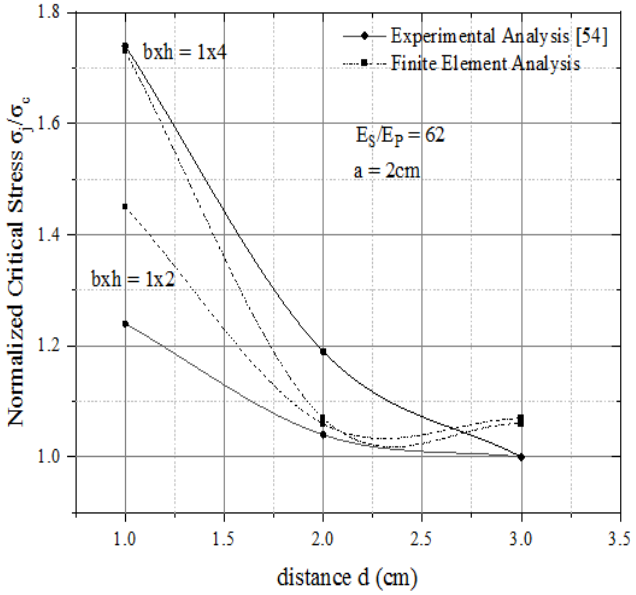

FIGURE 7: Normalized critical stress versus distance d for steel rectangular patch and a=2cm.

Size and location of the patches also have a significant influence on the critical stresses. As the patch size is doubled, the critical stresses for panels differs for each patch. For instance, with aluminum and steel patches, the critical stresses would increase 50% and 15%, respectively, at a=1cm and d = 1 cm. Plotted in Fig. 8 are the stress ratio σ_j/σ_c versus the thickness ratio of the patch t_j/t_p. Except for the initial rise of gain in stiffness, the effect tapers off quickly. This means that any further increase in patch thickness would not increase the critical stress.

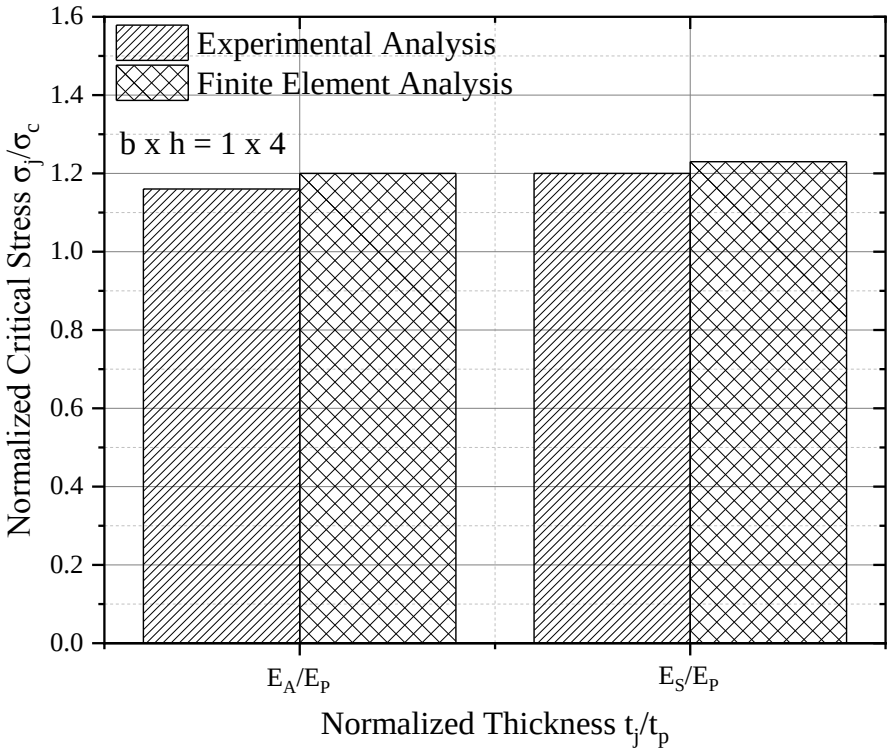

FIGURE 8: Normalized critical stress versus normalized thickness of rectangular patch for two different materials and a=1cm.

4.2 Rectangular Patches: Crack Trajectories and Instability

Since the geometry and material are symmetric across the crack plane, crack is expected to propagate straight ahead. The straight path of the crack tip which appears in macroscale, is practically insensitive in any small fluctuations and possible multi-branching, which are took place in microscale and can owe in the irregularities of microstructure. Even small imperfections by the manufacture of initial crack tip, do not influence the rectilinear trajectory propagation of crack tip [54].

Fig. 9 plots the strain energy density function as a function of the distance r ahead of the crack for d = 1 and 2 cm, where dW/dV would decrease with increasing distance from the crack. Displayed in Figs. 10 and 11 are results for the instability index as a function of the distance for a = 1 and 2 cm, respectively. In both cases, l tends to increase monotonically. This means that crack instability would increase with the distance d. The same is found for both the aluminum and steel patch. Fig. 12a, b shows the constant contours of dW/dV for the edge crack panel without any patches with a = 1 cm. The point G lies inside of the specimen (finite element result). This implies that stable crack propagation prevails regardless of loading rate as verified by experiments. If a patch is bonded to the specimen with the inner edge at d = 3 cm while the other edge is 1 cm from the outer edge of specimen. In this case, G is found to be at a distance 2.9cm from the crack tip (Fig. 12b). If the load increases further, the crack trajectory will run around the perimeter of the reinforcement patch. Similar, results will be displayed by moving the same patch closer to the crack tip, at d = 2 cm. In this case, it would tend to increase the intensity of the local energy intensity and moves G away from a straight path (Fig. 13).

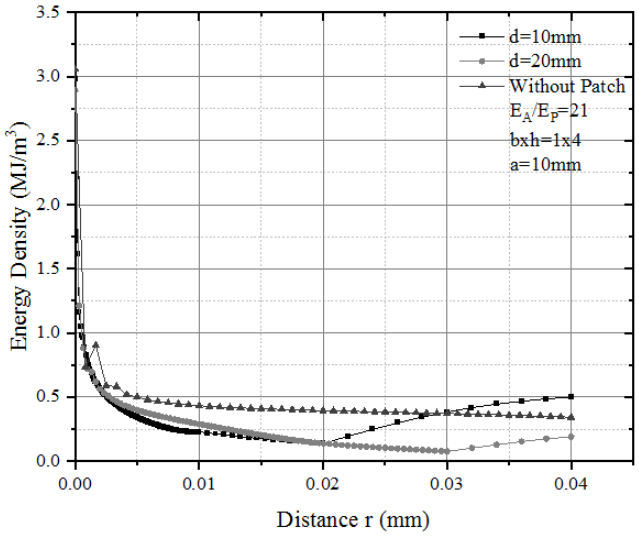

FIGURE 9: Strain energy density discontinuity across path for bonded aluminium patch (doted-line curve without patch).

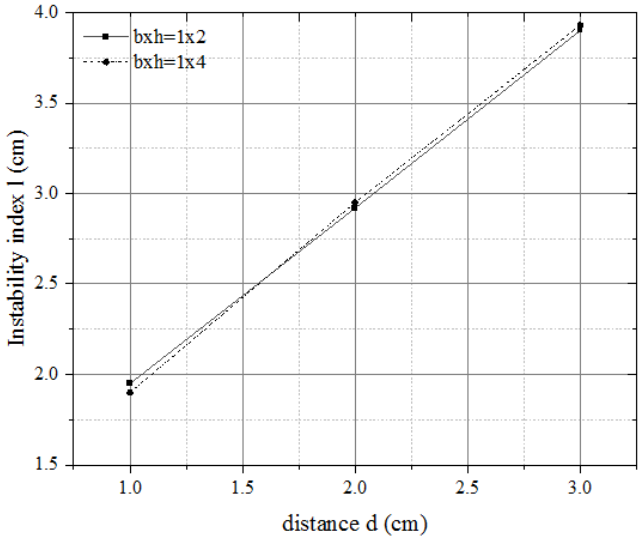

FIGURE 10: Variation of instability index l with distance d for rectangular patch with a=1cm (aluminium).

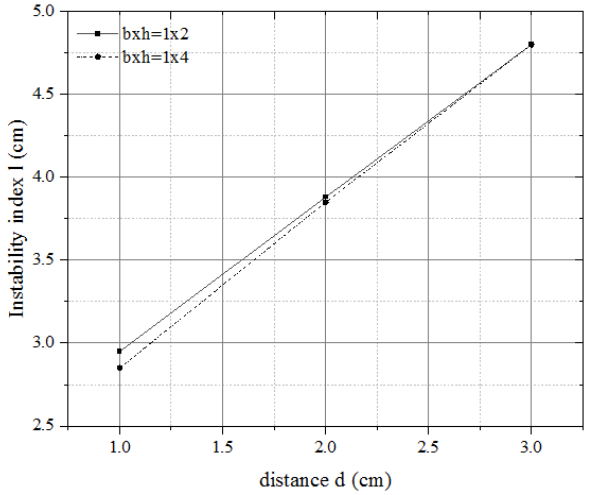

FIGURE 11: Variation of instability index l with distance d for rectangular patch with a=2cm (aluminium).

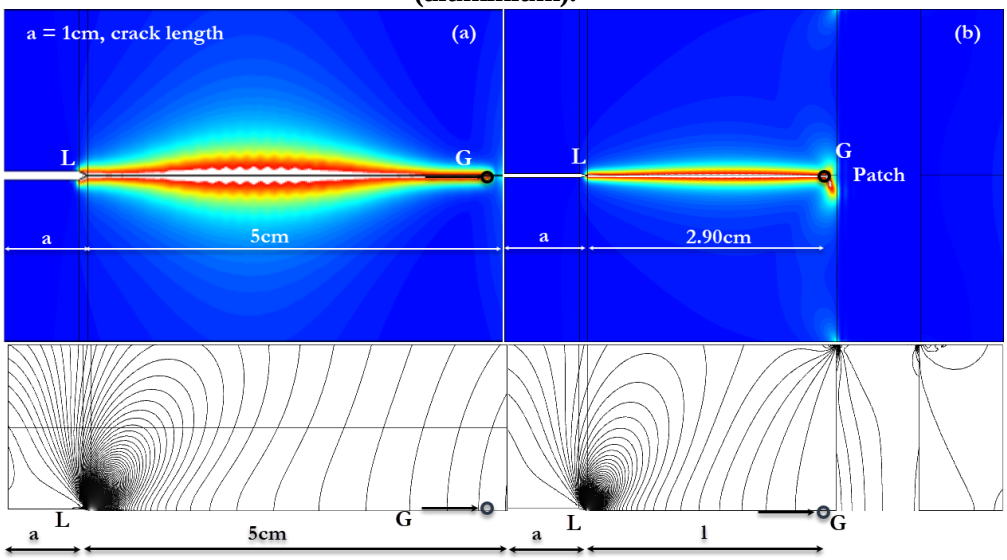

FIGURE 12: (a) Constant contours of strain energy for edge-cracked panel (a) without patch and a=1cm (b) with steel rectangular (bxh=1x4) patch with d=3cm and a=1cm-Damage representation.

Furthermore, the damage of the specimen tends to move away from the patch (R) before the lower corner (fig. 13). This was observed by tests where the crack would curve followed by complete fracture of the specimen. In that case, the curved trajectory will be unstable and perhaps not unique. It is clear that until the critical point (fig. 13) the crack propagates stably but when begins the divergence of the tip from its original axis, then is moved more rapidly, and also with unstable way. Figs. 14a and b exhibit the location of G for patches with size 1 x 2 cm^2 and 1 x 4 cm^2, respectively, at the same location d = 1 cm.

Note that G is shown to be at the boundary of the patch for both figures 14a and b where the crack, again, tends to run around the edge of the patch. These predictions from the strain energy density theory were observed also during experimental procedures. The curved trajectory which arises, generally is unstable but for small values ratio (H/W), this tend to become stable. The foregoing results for the aluminum and steel patches are summarized in Tables 3 and 4, respectively.

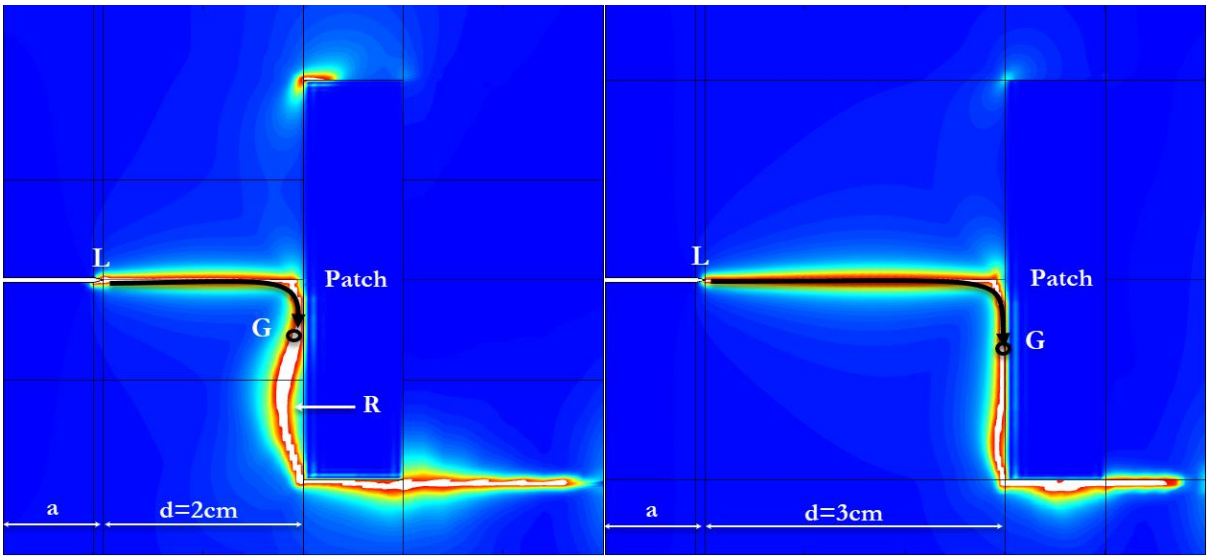

FIGURE 13: Damage for edge-cracked panel with steel rectangular patch (bxh=1x4, a=1cm) with d=2cm and d=3cm, respectively.

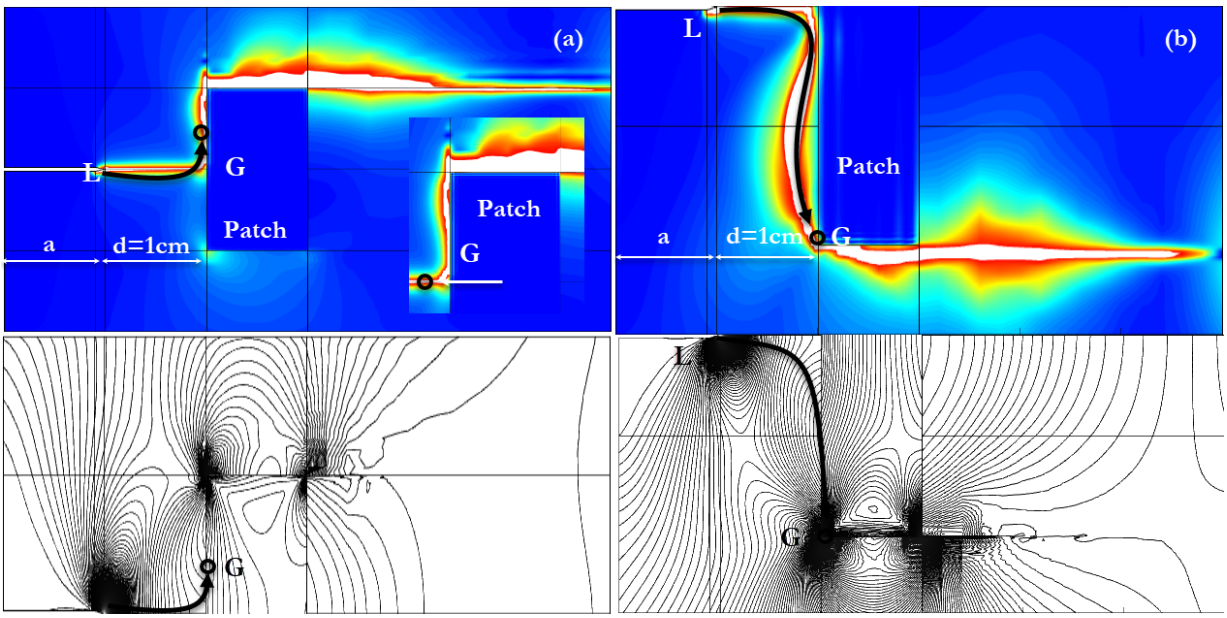

FIGURE 14: (a) Constant contours of strain energy for edge-cracked panel (a) with aluminium rectangular patch (bxh = 1x2) with d=1cm and a=1cm(b) with aluminium rectangular patch (bxh=1x4) patch with d=1cm and a=1cm-Damage representation.

TABLE 3
INSTABILITY INDEX FOR STEEL PATCH WITH E_S/E_P=21.

d (cm)	b x h = 1 x 2 cm^2		b x h = 1 x 4 cm^2	
a=1cm	l (cm)	Crack Path	l (cm)	Crack Path
1	1.95	Curve	1.90	Curve
2	2.75	Curve	2.95	Curve
3	3.90	Straight	3.93	Curve
a=2cm				
1	2.95	Curve	2.85	Curve
2	3.98	Straight	3.85	Straight
3	4.80	Straight	4.80	Straight

TABLE 4
INSTABILITY INDEX FOR STEEL PATCH WITH E_S/E_P=62

d (cm)	b x h = 1 x 2 cm^2		b x h = 1 x 4 cm^2	
a=1cm	l (cm)	Crack Path	l (cm)	Crack Path
1	1.85	Curve	1.60	Curve
2	2.82	Curve	2.92	Curve
3	3.83	Straight	3.90	Curve
a=2cm				
1	2.90	Curve	2.80	Curve
2	3.80	Curve	3.95	Curve
3	4.80	Straight	4.80	Straight

4.3 Semi-Annular Patches: Critical Stresses

Shown in Figs. 15 and 16 are decrease of the normalized critical stresses with the distance d for initial crack length a = 1 and 2 cm, respectively. It can be seen from these results that considerable gain in the critical stress level can be realized for the steel patch by having it near to the crack. At about d = 3 cm, the effect of the path tends to diminish. The influence of the patch thickness on the critical stress is illustrated in Fig. 17. The initial gain tapers off with continuous increase in t_A and t_S, a result that is similar to the rectangular patch and is to be expected.

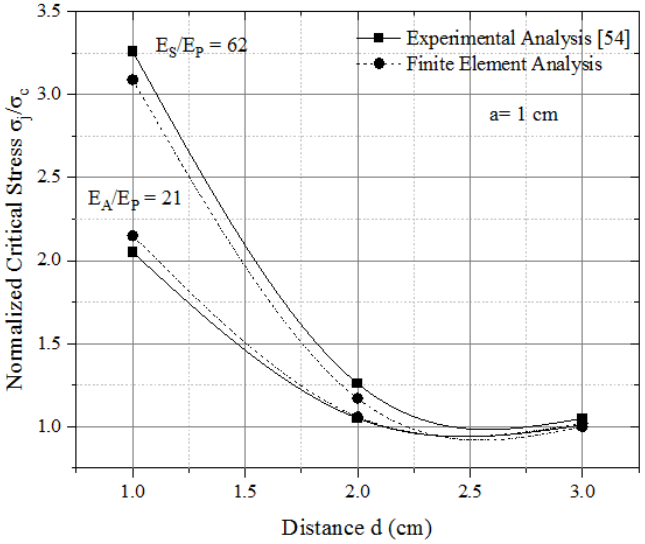

FIGURE 15: Comparison of predicted normalized critical stress versus distance d for semi annular patch for a=1cm.

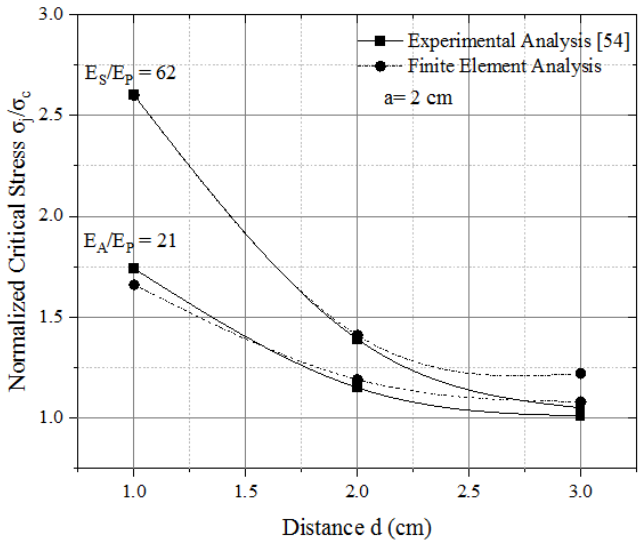

FIGURE 16: Comparison of predicted normalized critical stress versus distance d for semi annular patch for a=2cm.

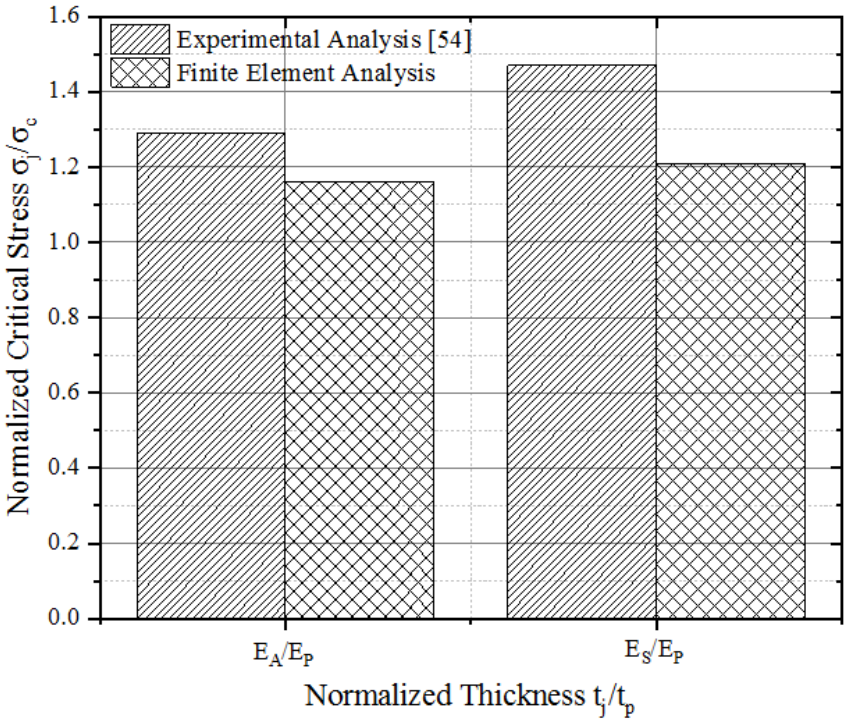

FIGURE 17: Normalized critical stress versus normalized thickness of semi annular patch for two different materials and a=1cm.

4.4 Semi-Annular Patches: Crack Trajectory and Instability Index

For a = 1 cm, Fig. 18 shows that rises with d and is independent of the material of the patches. A small difference for the aluminum and steel path is observed as the initial crack length is increased to 2 cm. This is shown in Fig. 19. Contours of constant dW/dV are displayed in Fig. 20 for a = 1 cm and d = 2 cm. In this case, G remains on the axis of symmetry with l= 1.80 cm. Similar results are found for d = 1 and 3 cm and a = 2 cm and hence no further discussions are required. Refer to Table 5 for different value of the instability index. Similar results are found for d = 1 and 3 cm and a = 2 cm and hence no further discussions are required. Refer to Table 5 for different value of the instability index.

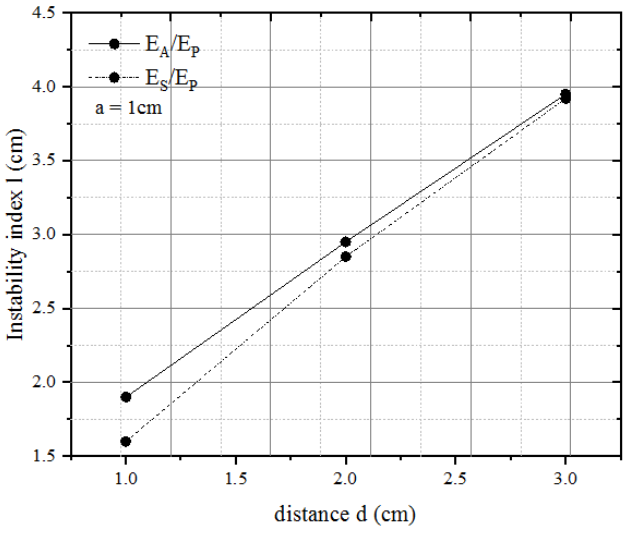

FIGURE 18: Variation of instability index l with distance d for semi annular patch and a=1cm

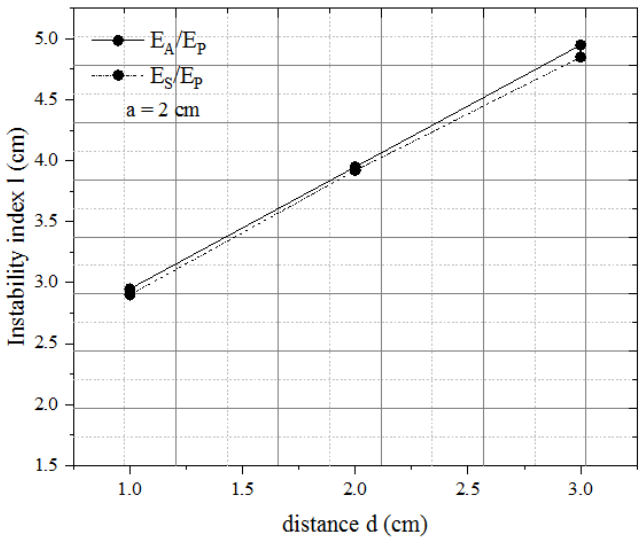

FIGURE 19: Variation of instability index l with distance d for semi annular patch and different materials with a=2cm.

TABLE 5
INSTABILITY INDEX FOR ALUMINIUM AND STEEL PATCH

d (cm)	b x h = 1 x 2 cm^2		b x h = 1 x 4 cm^2	
a=1cm	l (cm)	Crack Path	l (cm)	Crack Path
1	0.90	Straight	0.62	Straight
2	1.80	Straight	1.90	Straight
3	2.80	Straight	2.80	Straight
a=2cm				
1	0.90	Straight	0.90	Straight
2	1.92	Straight	1.90	Straight
3	2.90	Straight	2.92	Straight

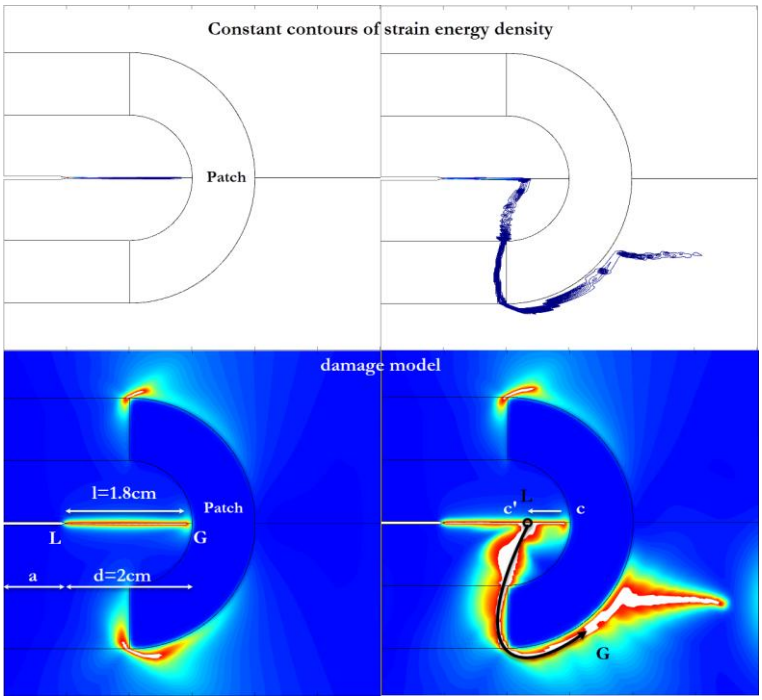

FIGURE 20: Constant contours of strain energy density for edge cracked panel with steel semi annular patch with d=2cm and a=1cm.

V. CONCLUSIONS

This work has conclusively proven that the instability index can be used as an indicator of the effectiveness of reinforcement to arrest a crack. Several parameters, such as geometric and materials of the patch alters effectively is the intensity of the load transferred to the crack tip region and hence the crack growth characteristics. Broadly translated our findings indicate that the edge crack specimen gives rise to unstable fracture under uniform tensile loading. However, the kind of the crack propagation, depends on the rate and the way of loading of the specimen from the test machine, namely, whether the increase of the imposed displacement or the force respectively, will be controlled.

The evidence from this study that, for low local energy intensity of the rectangular patch specimens, the initial crack runs straight and arrests at the patch edge regardless of the initial crack length and position. However, as the patch is moved closer to the crack tip crack path deviated from the straight line (critical point). This occurred for the rectangular patches regardless of the other variables. A temporary arrest of extension is presented at point G, but with furthermore increasing of the loading, leaded to catholic fracture. Moreover, the crack trajectory was straight for the semi-annular patch even when patch distance from the crack tip is increased, a new crack trajectory was observed. This is independent of the geometrical characteristics of the specimen, as well as, the initial crack length. Nevertheless, the crack tip is still trapped inside the semi-annular patch for a certain load. Our work has led us to conclude that, we can direct to a certain point outside the patch zone. That means, a further investigation of the method of Hypothesis of the Maximum Gradient of the Strain Energy Density (HMG of SED)

must be investigated. The most important limitation lies in the fact that this method provides great accuracy only in a small-scale specimen. It is also recommended that further research should be undertaken in the area of ductile materials.

REFERENCES

[1] G.C. Sih, "Introductory chapters, in: Mechanics of Fracture, Vols. I to VII," ed. G.C. Sih, MartinusNijhof, The Netherlands, pp. 1972-1982.

[2] G.C. Sih, "Fracture mechanics of engineering structural component, in: Fracture Mechanics Technology," eds., G.C. Sih and I. Faria, MartinusNijhof, The Netherlands, pp. 35-101, 1984.

[3] Schijve, J., "Crack stoppers and ARALL laminates," Engineering Fracture Mechanics, vol. 37, issue 2, pp. 405–421, 1990. doi:10.1016/0013-7944(90)90050-Q

[4] M. B.Heinimann, , R. J.Bucci, M.Kulak and M. Garratt, "Improving damage tolerance of aircraft structures through the use of selective reinforcement," Proceedings of the 23rd Symposium of the International Committee on Aeronautical Fatigue, DGLR, Munich, Germany, pp. 197–208, June 2005.

[5] X. Zhang and Y. Li, "Damage tolerance and fail safety of welded aircraft wing panels," AIAA Journal, vol. 43, issue 7, pp. 1613–1623, 2005. doi:10.2514/1.10275

[6] M. Colavita, A. Bowler, X. Zhang and P. E. Irving, "Adhesively bonded CFRP straps as fatigue crack growth retarders on AA2024-T3," Proceedings of SAMPE Conference 2006, ASM, vol. 13C, Corrosion: Environments and Industries, http://www.sampe.org/store/paper.aspx?pid=3542, April 2006.

[7] A. Bowler "Crack stoppers and fail safety in integral metal aircraft structure," Master's Thesis, Cranfield University, England, U.K., 2005.

[8] P. Colombi, A. Bassetti and A. Nussbaumer, "Delamination effects on cracked steel members reinforced by prestressed composite patch," Theoretical and Applied Fracture Mechanics, vol. 39, issue 1, pp. 61–71, 2003.doi:10.1016/S0167-8442(02)00138-6

[9] A. Baker, "Crack patching: Experimental studies, practical applications," Bonded Repair of Aircraft Structures, edited by A. Baker and R. Jones, Martinus–Nijhoff, Dordrecht, The Netherlands/Boston, pp. 107–173, 1988.

[10] A. Baker, "Fibre composite repair of cracked metallic aircraft components–Practical and basic aspects," Composites, vol. 18, issue 4, pp. 293–308, 1987. doi:10.1016/0010-4361(87)90293-X

[11] R. Jones and R. J. Callinan, "Finite element analysis of patched cracks," Journal of Structural Mechanics, vol. 7, issue. 2, pp. 107–130, 1979.

[12] S. Naboulsi and S. Mall, "Modelling of a cracked metallic structure with bonded composite patch using the three layer technique," Composite Structures, vol. 35, issue 3, pp. 295–308, 1996. doi:10.1016/0263-8223(96)00043-8

[13] C. T. Sun, J. Klung and C. Arendt, "Analysis of cracked aluminum plates repaired with bonded composite patches," AIAA Journal, vol. 34, issue 2, pp. 369–374, 1996.

[14] L. Rose, "A cracked plate repaired by bonded reinforcements," International Journal of Fracture, vol. 18, issue 2, pp. 135–144, 1982. doi:10.1007/BF00019638

[15] V. Sabelkin, S. Mall, J. B. Avram, "Fatigue crack growth analysis of stiffened cracked panel repaired with bonded composite patch," Engineering Fracture Mechanics, vol. 73, issue 11, pp. 1553–1567, 2006. doi:10.1016/j.engfracmech.2006.01.029

[16] A. A. Baker, "Bonded composite repair for fatigue-cracked primary aircraft structure,"CompositeStructtures, vol. 47, pp. 431-443, 1999.

[17] V. R. S. Turaga and S. Ripudaman, "Modelling of patch repairs to a thin cracked sheet, " Engineering Fracture Mechanics, vol. 62, issue 2-3 pp. 267-289, 1999.

[18] W. H. Chen and S. H. Yang, " Estimation of stress intensity factors in partially patched cracked composite laminates by multiplayer hybrid-stress finite element method, " Finite Element Analysis and Design, vol. 21, pp. 21-44, 1998.

[19] R. Jones and W. K. Chiu, "Composite repairs to crack in metallic components," Composite Structures, vol. 44, pp. 17–29, 1999.

[20] E. Belason, ''Bonded doublers for aircraft structure repair,'' Aerospace Engineering, pp. 13 – 18, 1995.

[21] J. H. Park, T. Ogiso and S. N. Atluri, ''Analysis of cracks in aging aircraft structures, with and without composite-patch repairs,'' Computational Mechanics, vol. 10, issue 3-4, pp. 169 – 201, 1992.

[22] G. C. Sih and R. C. Chu, ''Characterization of material inhomogeneity by stationary values of strain energy density,'' Theoretical Applied Fracture Mechanics, vol. 5 151-161, 1986.

[23] A. Shukla, R. Desantis, B. Gauthier, ''Crack arrest with externally bonded ligaments,'' Mechanics Research Communication, vol. 13, issue 1, pp.25-31, 1986.

[24] E. E Gdoutos and D. A. Zacharopoulos, ''Mixed-mode crack growth in plates under three-point bending,'' Experimental Mechanics, vol. 27, pp. 365-369, 1987.

[25] G. C. Sih and C. H. Chue, ''Stability and integrity of mechanical joints in sight vehicles: Local and global energy density,'' Theoretical Applied Fracture Mechanics, vol. 10, pp. 135-149, 1988.

[26] G. C. Sih and T. B. Hong, ''Integrity of edge-debonded patch on cracked panel,'' Theoretical Applied Fracture Mechanics, vol. 12, pp. 121-139, 1989.

[27] C. K. Chao and J. J. Shie, ''Stability of failure initiation by fracture for a bimaterial body with an edge crack, '' Theoretical Applied Fracture Mechanics, vol. 14, pp.123-133, 1990.

[28] C. K. Chao and S.Y. Lin, ''Failure stability of a cracked layer between dissimilar materials, '' Theoretical Applied Fracture Mechanics, vol. 13, pp. 59-68, 1980.

[29] D.A. Zacharopoulos, ''Study of fracture instability in brittle materials by strain energy density, '' Fracture Behaviour and Design of Materials and Structures, 8th Biennial European Conference on Fracture, I, pp. 112-117, 1990.

[30] C. H. Chue and Y. D. Wei, ''Failure initiation sites and instability of structural components with localized energy density,'' Theoretical Applied Fracture Mechanics, vol. 15, pp. 163-177, 1991.

[31] G. C. Sih, ''Mechanics of failure initiation and propagation'', Kluwer Academic Publishers, The Netherlands, 1991.

[32] B. Bachir Bouiadjra, H. Fekirini, M. Belhouari, B. Serier, B. Benguediab and D. Ouinas, ''SIF for double- and single-sided composite repair in mode I and mixed mode, '' Journal of Reinforcement Plastic and Composites, vol. 29, issue 10, pp. 1463-1475, 2009. doi:10.1177/0731684409102836.

[33] D. Ouinas, B. Bachir Bouiadjra, B. Achour and N. Benderdouche, ''Modelling of a cracked aluminium plate repaired with composite octagonal patch in mode I and mixed mode,'' Materials and Design, vol. 30, pp. 590-595, 2009.

[34] L. Aminallah, T. Achour, B. Bachir Bouiadjra, B. Serier, A. Amrouche and X. Feaugas et al., ''Analysis of the distribution of thermal residual stresses in bonded composite repair of metallic aircraft structures,'' Computational Materials Science, vol. 49, pp. 1023-1027, 2009.

[35] D. Ouinas, M. Sahnoune, N. Benderdouche and B. Bachir Bouiadjra, ''Stress intensity factor analysis for notched cracked structure repaired by composite patching,'' Materials and Design, vol. 30, pp. 2302-2308, 2009.

[36] B. Bachir Bouiadjra, H. Fekirini, M. Belhouari and B. Serier, ''Numerical analysis of the behaviour of repaired inclined cracks with bonded composite patch having two adhesive bands in aircraft structures,'' Proceedings of the Institution of Mechanical Engineers Part G: Journal of Aerospace Engineering, vol. 222, pp. 963-968 2008.

[37] H. Fekirini, B. Bachir Bouiadjra, M. Belhouari, B. Boutabout and B Serier, ''Numerical analysis of the performances of bonded composite repair with two adhesive bands in aircraft structures,'' Composite Structures, vol. 82, pp. 84-89, 2008.

[38] M. Bezzerrouki, B. Bachir Bouiadjra and D. Ouinas, ''SIF for cracks repaired with single composite patch having two adhesive bands and double symmetric one in aircraft structures,'' Computational Materials Science, vol. 44, pp. 542-546.

[39] D. Ouinas, B. B. Bouiadjra and B. Serier, ''The effects of disbonds on the stress intensity factor of aluminium panels repaired using composite materials,'' Composite Structures, vol. 78, pp. 278-284, 2007.

[40] K. Madani, S. Touzain, X. Feaugas, M. Benguediab and M. Ratwani, ''Stress distribution in a 2024-T3 aluminum plate with a circular notch, repaired by a graphite/epoxy composite patch,'' International Journal of Adhesion and Adhesives, vol. 29, pp. 225-233, 2009.

[41] B. Bachir Bouiadjra, M. Belhouari and B. Serier, ''Computation of the stress intensity factor for repaired crack with bonded composite patch in mode I and mixed mode,'' Composite Structures, vol. 56, pp. 401-406, 2002.

[42] B. Bachir Bouiadjra, T. Achour, M. Berrahou, D. Ouinas and X. Feaugas,''Numerical estimation of the mass gain between double symmetric and single bonded composite repairs in aircraft structures,''Materials and Design, vol. 31, pp. 3073-3077, 2010.

[43] B. Bachir Bouiadjra, H. Fekirini, B Serier and M. Benguediab,''Numerical analysis of the beneficial effect of the double symmetric patch repair compared to single one in aircraft structures,'' Computational Material Science, vol. 38, pp. 824-829, 2007.

[44] B. Bachir Bouiadjra, H. Fekirini, B. Serier, M. Belhouari and M. Benguediab, ''Energy release rate for repaired inclined cracks with bonded composite patch having two adhesive bands in aircraft structures,''Journal of Reinforced Plastics and Composites, vol. 27, pp. 1135-1145, 2008

[45] B. Bachir Bouiadjra, H. Fekirini, B. Serier and M. Benguediab,''SIF for inclined cracks repaired with double and single composite patch, '' Mechanics of Advanced Materials Structures, vol. 14, pp. 303-308, 2007.

[46] T. Achour, B. Bachir Bouiadjra and B. Serier, ''Numerical analysis of the performances of the bonded composite patch for reducing stress concentration and repairing cracks at notch,'' Computational Material Science, vol. 28, pp. 41-48, 2003.

[47] M. Belhouari, B. Bachir Bouiadjra, M. Megueni and K. Kaddouari, ''Comparison of double and single bonded repairs to symmetric composite structures: a numerical analysis,'' Composite Structures, vol. 65, pp. 47-53, 2004.

[48] D. Ouinas and A. Hebbar, B. Bachir Bouiadjra, M. Belhouari and B. Serier, ''Numerical analysis of the stress intensity factors for repaired cracks from a notch with bonded composite semicircular patch,'' Composites Part B, vol. 40, pp. 804-810, 2009.

[49] D. Ouinas, B. Bachir Bouiadjra, B. Serier B and S. M. Bekkouche, ''Comparison of the effectiveness of boron/epoxy and graphite/epoxy patches for repaired cracks emanating from a semicircular notch edge,'' Composite Structures, vol. 80, pp. 514-522.

[50] D. Ouinas, B. Serier and B. Bachir Bouiadjra, ''The effects of disbands on the pure mode II stress intensity factor of aluminium plate reinforced with bonded composite materials,'' Computational Material Science, vol. 39, pp. 782-787, 2007.

[51] B. Bachir Bouiadjra, M. Belhouari and B. Serier, ''Computation of the stress intensity factors for patched cracks with bonded composite repairs in mode I and mixed mode,'' Composite Structures, vol. 56, pp. 401-406, 2002.

[52] T. Ting, R. Jones, W. K. Chiu, I. H. Marshall and J. M. Greer, ''Composites repairs to rib stiffened panels,''Composite Structures, vol. 47, pp. 737-743, 1999.

[53] B. Bachir Bouiadjra, H. Fekirini, B. Serier and M. Benguediab, ''SIF for inclined cracks repaired with double and single composite patch,'' Mechanics of Advanced Materials and Structures, vol. 14, pp. 303-308, 2007.

[54] D. A. Zacharopoulos, ''Arrestment of cracks in plane extension by local reinforcements,'' Theoretical and Applied Fracture Mechanics, vol. 32, pp. 177-188, 1999.

[55] D. A. Zacharopoulos, ''The complication of crack path and its kind under mode-I loading: The case of the DCB specimen'' Theoretical and Applied Fracture Mechanics, vol. 97, pp. 426-433, 2018.

[56] G. C. Sih and E. Baisch, ''Angled crack growth estimate with overshoot and/or overload,'' Theoretical and Applied Fracture Mechanics, vol. 18, pp. 31-45, 1992.

[57] Comsol Multiphysics, version 5.6.